Quantitative analysis of nucleotide modulation of DNA binding by DnaC protein of *Escherichia coli*

Subhasis B. BISWAS[1], Stephen FLOWERS and Esther E. BISWAS-FISS[2]

Department of Molecular Biology, School of Medicine, Graduate School of Biomedical Sciences, University of Medicine and Dentistry of New Jersey, Stratford, NJ 08084, U.S.A.

In this study, we have presented the first report of *Escherichia coli* DnaC protein binding to ssDNA (single stranded DNA) in an apparent hexameric form. DnaC protein transfers DnaB helicase onto a nascent chromosomal DNA replication fork at *oriC*, the origin of *E. coli* DNA replication. In eukaryotes, Cdc6 protein may play a similar role in the DNA helicase loading in the replication fork during replication initiation at the origin. We have analysed the DNA-binding properties of DnaC protein and a quantitative analysis of the nucleotide regulation of DnaC–DNA and DnaC–DnaB interactions using fluorescence anisotropy and affinity sensor analysis. DnaC protein bound to ssDNA with low to moderate affinity and the affinity was strictly modulated by nucleotides. DnaC bound ssDNA in the complete absence of nucleotides. The DNA-binding affinity was significantly increased in the presence of ATP, but not ATP[S]. In the presence of ADP, the binding affinity decreased approximately fifty-fold. Both anisotropy and biosensor analyses demonstrated that with DnaC protein, ATP facilitated ssDNA binding, whereas ADP facilitated its dissociation from ssDNA, which is a characteristic of an ATP/ADP switch. Both ssDNA and nucleotides modulate $DnaB_6 \cdot DnaC_6$ complex formation, which has significant implications in DnaC protein function. Based on the thermodynamic data provided in this study, we have proposed a mechanism of DnaB loading on to ssDNA by DnaC protein.

Key words: DnaC protein, DnaB helicase, DNA replication, DNA binding, initiation, origin of replication.

INTRODUCTION

In *Escherichia coli*, three proteins, DnaA, DnaB, and DnaC, are required for the initiation of DNA replication at *oriC*, the chromosomal origin of replication [1–5]. DnaA is the initiator protein that binds to three AT-rich repeats in *oriC* and creates a partial opening of duplex DNA that allows the DnaB • DnaC protein complex to associate with the partially unwound origin [6]. Nevertheless, it is still unclear how DnaB helicase loads on to the open complex, and what the role of DnaC protein in the loading process is. The DnaB protein is a hexamer that acts as the chromosomal replicative helicase, whereas DnaC is required for both modulation of the activities and assisting DnaB helicase to bind to ssDNA (single stranded DNA) at the origin [7–12]. Therefore, DnaC protein has a pivotal role in initiation and DnaB helicase function. In *E. coli*, the origin of DNA replication is activated by multiple molecules of DnaA binding DnaA boxes in *oriC*, leading to opening of the origin and formation of an 'open complex' [6,13]. DnaA proteins in the open complex recruit DnaB • DnaC complex, presumably through a specific DnaA–DnaB interaction. DNA binding leads to ATP hydrolysis by the DnaB • DnaC complex and release of DnaC protein [14,15]. In bacteriophage λ, λP protein replaces DnaC and assists DnaB helicase to bind λori (the origin of λ DNA replication) that requires first activation by the λ initiator protein, λO [16–18]. In eukaryotes, proteins with very similar functions play these roles [19–23]. In the yeast, *Saccharomyces cerevisiae*, Cdc6 protein assists MCM (minichromosome maintenance) proteins, that appear to act as a DNA helicase in binding to the origin of replication which is, in turn, activated by the origin recognition complex (ORC) [24–27]. Therefore, in its unique role, DnaC protein appears to be a prototype for both prokaryotic and eukaryotic organisms.

DnaC protein of *E. coli* is a 29 kDa monomeric protein [28,29]. With DnaB helicase, it forms a six-to-six complex resulting in the $DnaB_6 \cdot DnaC_6$ complex, and the three-dimensional structure of this complex has been revealed by cryo-electron microscopy [30–32]. We have shown previously by ultraviolet photo-crosslinking studies, that DnaC protein binds ATP and that it first forms a $DnaB_6 \cdot DnaC_6 \cdot$ ATP dead-end ternary complex in which the ATPase activity of DnaB is attenuated [9].

Studies by Learn et al. [17] indicated alterations in the DNA-binding properties of DnaB helicase in the presence of DnaC or λP proteins. It has been shown that the release of DnaC or λP from the ternary complex is required for rejuvenation of the DnaB ATPase and its coupled DNA helicase activities. Therefore, the $DnaB_6 \cdot DnaC_6 \cdot$ ATP ternary complex first interacts with ssDNA, which is followed by activation of its ATPase and DNA helicase activities. However, it is not clear whether DnaC protein alone can bind ssDNA. Direct DNA-binding studies, such as electrophoretic mobility-shift assays, did not demonstrate DNA binding by DnaC protein [17]. A recent report on the mechanism of DNA helicase loading in *Bacillus subtilis* demonstrated a somewhat altered mechanism of helicase loading, involving an additional loader protein, in addition to DnaC and DnaA proteins that are involved in *E. coli* [33]. In addition, we have recently demonstrated that DnaC protein, DnaB helicase, and DnaG primase can form an assembly on short single-stranded oligonucleotides, and synthesize primers that were shorter in the presence of DnaC [34].

In order to fully delineate the interactions of DnaC protein with ssDNA templates, we have quantitatively characterized the

Abbreviations used: DnaBW48, a single-tryptophan mutant of DnaB; DTT, dithiothreitol; IPTG, isopropyl β-D-thiogalactoside; ssDNA, single stranded DNA; *oriC*, the origin of *Escherichia coli* DNA replication; k_{on}, association rate constant; ORC, origin recognition complex; Fl-oligo$(dT)_{25}$, 5′-fluorescein-labelled 25 nucleotides single stranded oligo$(dT)_{25}$; m*A*, milli anisotropy (units); PBST, PBS containing 0.05 % Tween 20.

[1] To whom correspondence should be addressed (e-mail subhasis.biswas@umdnj.edu).

[2] Present address: Department of Bioscience Technologies, Thomas Jefferson University, Philadelphia, PA 19107, U.S.A.

DNA-binding properties of DnaC protein with DNA, under a variety of conditions, using a combination of fluorescence anisotropy [35–38] and biosensor analysis [39,40]. Boyer et al. [36] have elegantly demonstrated that fluorescence anisotropy is a unique tool for complete thermodynamic analysis of protein–DNA interactions using a wide variety of DNA-binding proteins and DNA substrates. We have utilized previously the precision of this technique for studying the interactions of *E. coli* DNA primase with DNA [41].

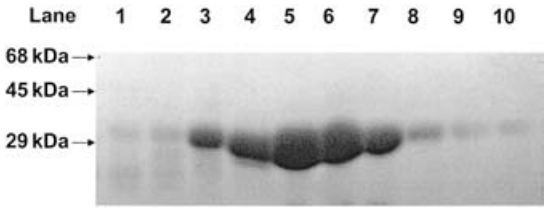

Figure 1 SDS/PAGE of DnaC

DnaC was purified through gel filtration. Aliquots of the peak fractions were loaded on the gel. The gel was electrophoresed and stained with Coomassie Brilliant Blue R-250. Lanes 1–10 represent fractions 46–55 respectively.

MATERIALS AND METHODS

Nucleic acids and other reagents

Radiolabelled and unlabelled oligonucleotides were both purchased from Sigma-Genosys (Cambridge, U.K.) and Fisher Chemicals (Pittsburgh, PA, U.S.A.). Radiolabelled single stranded oligonucleotides were covalently linked with either the fluorescein probe [Fl-oligo$(dT)_{25}$] or biotin [biotin-oligo$(dT)_{30}$] at the 5′ end. All other reagents used in this study were ACS reagent or spectroscopy grade and obtained from Aldrich Chemical Co., (Milwaukee, WI, U.S.A.). HPLC-grade water was obtained from Fisher Chemicals (Pittsburgh, PA, U.S.A.). Chemicals for fluorescence measurements were purchased from Panvera Corporation (Milwaukee, WI, U.S.A.).

Buffers

Lysis buffer [25 mM Tris/HCl (pH 7.5), 10 % sucrose and 250 mM NaCl]. Buffer A [25 mM Tris/HCl (pH 7.5), 5 mM $MgCl_2$, 5 mM dithiothreitol (DTT) and 10 % (v/v) glycerol]. Buffer B [20 mM Hepes/NaOH (pH 7.5), 5 mM $MgCl_2$, 5 % (v/v) glycerol, 5 mM DTT and 50 mM NaCl], or as indicated. Buffers for fluorescence anisotropy and biosensor measurements were prepared with HPLC-grade water, fluorescence grade reagents, and filtered through a 0.2 micron nitrocellulose filter. Buffers were examined for background fluorescence before use in anisotropy measurements.

DnaC expression and purification

DnaC gene was amplified by PCR using plasmid pJK101 containing wild-type DnaC gene, obtained as a gift from Dr Joan Kobori and Dr Arthur Kornberg of Stanford University, Palo Alto, CA, U.S.A. [28]. The amplified gene was inserted into a pET29b vector (Novagen Inc., Madison, WI, U.S.A.) under the control of a T7 promoter (pET29b-DnaC recombinant plasmid) and confirmed by DNA sequencing. DnaC was purified from *E. coli* BL21 (DE3) strain harbouring the pET29b-DnaC plasmid. *E. coli* cells were grown in 6-litre batches in 2YT medium [1.6 % (w/v) tryptone, 1 % (w/v) yeast extract, 0.5 % (w/v) NaCl] containing 50 μg/ml kanamycin at 37 °C to a D_{600} of 0.4. At this point, IPTG (isopropyl β-D-thiogalactoside) was added to a final concentration of 0.1 mM. The cells were grown for an additional 4 h and then harvested by centrifugation at 7740 ***g*** (8000 rev./min) for 10 min. The cell pellet was resuspended in lysis buffer and frozen at − 80 °C. Cells were thawed on ice and lysed using 0.2 mg/ml lysozyme, 5 mM $MgCl_2$, 2 mM spermidine, 250 mM NaCl and 5 mM DTT by incubating on ice for 60 min. This was followed by a 5 min incubation at 37 °C. The mixture was homogenized on ice followed by sonication. The resulting lysate was incubated, after increasing NaCl concentration to 750 mM, for 1 h on ice while shaking.

The lysate was centrifuged at 41 400 ***g*** (18 500 rev./min) for 30 min at 4 °C. The supernatant was precipitated using 0.26 g/ml ammonium sulphate for 2 h on ice followed by centrifugation at 41 400 ***g*** for 30 min. The protein was purified first by DEAE-Sepharose chromatography (AP Biotech, Piscataway, NJ, U.S.A.). The protein was then purified by HPLC gel filtration using a preparative Bio-Rad TSK250 gel filtration column (1.6 cm × 60 cm stainless steel). Peak fractions were collected and concentrated using ultrafiltration (Figure 1). Protein homogeneity was 99 %, as determined by SDS gel electrophoresis, and the concentration was determined by UV absorption at 280 nm ($\varepsilon_{280} = 2.3 \times 10^5\ M^{-1} \cdot cm^{-1}$).

Steady-state fluorescence and anisotropy measurements

Fluorescence anisotropy measurements were performed on a custom-made photon-counting spectrofluorometer equipped with a 300 W Xenon arc lamp as power source, dual Hamamatsu R928P photo-multiplier tubes and computer controlled Glan–Thompson quartz polarizers. Excitation and emission slits were adjusted at 8 nm and 4 nm respectively. For fluorescein-labelled probes, the samples were excited at 488 nm and anisotropy was measured at 540 nm. Excitation and emission slits were adjusted at 8 nm and 4 nm respectively, for all anisotropy measurements.

The temperature was adjusted to 20 °C, by the use of a thermostat attached to the cell chamber, unless otherwise indicated. Intensity was measured in triplicate for 10 s and averaged. Anisotropy, *A*, is defined as:

$$A = (I_{vv} - G \times I_{vh})/(I_{vv} + 2 \times G \times I_{vh}) \quad (1)$$

where I_{vv}, I_{vh}, I_{hv} and I_{hh} represent the fluorescence signal for excitation and emission with the polarizers set at (0°,0°), (0°,90°), (90°,0°) and (90°,90°) respectively, and G is the instrument correction factor ($\equiv I_{hv}/I_{hh}$). The fluorescein-labelled oligonucleotide, oligo$(dT)_{25}$ was used as a probe. It was diluted in buffer B to a final concentration of 3.75×10^{-9} M and titrated with DnaC ranging in concentration from 3.5×10^{-8} to 7×10^{-6} M. For all DNA-binding studies, samples were excited at 488 nm and anisotropy was measured at 540 nm where smallest variation in the total fluorescence intensity was observed. Fluorescence intensities were measured for 3 × 10 s and averaged. Anisotropy values were expressed as milli-anisotropy or m*A*, which is equal to the measured anisotropy multiplied by 1000. The standard deviation for anisotropy values was ± 2 m*A*.

For DnaB–DnaC interactions, 160 nM DnaBW48, DnaC protein at indicated concentrations, appropriate nucleotides (100 μM) and/or oligo$(dT)_{25}$ were assembled in 1 ml total volume in buffer B. The mixture was incubated at 20 °C for 5 min and anisotropy was measured for 10 s in triplicate at the same temperature. For measurements involving tryptophan anisotropy, the excitation wavelength was 295 nm and the emission wavelength was set to 330 nm. The anisotropy data were analysed as described

in detail previously [36,37,41–43] using nonlinear regression analysis. The K_d is defined as the protein concentration at which half of the sites are occupied when the ligand concentration is constant.

IAsys biosensor analysis of DnaC • oligo(dT)$_{30}$ binding

DNA binding was performed using an IAsys affinity biosensor (Affinity Sensors, Cambridge, U.K.). Streptavidin- and biotin-labelled oligo(dT)$_{30}$ was immobilized on to a biotin cuvette according to manufacturer's instructions. The sensor chip was washed three times with 160 μl of PBS containing 0.05 % Tween 20 (PBST) and was allowed to equilibrate for 10 min. Baseline data were measured for a 3 min period. After the baseline had been established, 40 μl of a 2 mg/ml solution of streptavidin was added and binding was measured for 10 min. Next, the sensor chip was washed three times with 180 μl of PBST and 3 min of baseline was collected. Biotinylated oligo(dT)$_{30}$ was then added to the solution. Binding was allowed to occur for 5 min. The cuvette was then washed three times with PBST. Thereafter, the chip was ready to use in the DNA-binding studies described below.

Various amounts of DnaC in buffer B were pre-incubated in buffer B containing 50 mM NaCl for 5 min at 22 °C with nucleotide cofactors: 50 μM ATP, 50 μM ATP[S] or 50 μM ADP. Reactions were initiated by addition of pre-incubated DnaC protein to the cuvette and surface plasmon resonance response was recorded with a 5 s delay. In general, response data were collected for 5 min. After binding, DnaC was removed rapidly, the cuvette was washed with the binding buffer, and dissociation response was recorded for 3 min. The sensor chip was regenerated by the addition of 4 M NaCl for a 2 min period and then it was re-equilibrated with buffer B. Binding was analysed using the Fast fit software or PRISM 3.03 software from GraphPad Software for Science, San Diego, CA, U.S.A.

RESULTS

Escherichia coli DnaC protein binds to ssDNA with low affinity

We have shown previously that DnaC protein binds nucleotides by photo-crosslinking and demonstrated that it also binds ATP/dATP in the DnaB • DnaC complex [9]. The question we seek to answer here is: does DnaC protein bind DNA and form a stable DnaC • DNA complex? All previous studies directed toward resolving the hypothesized intrinsic DNA binding by DnaC protein, using electrophoretic mobility-shift assay, photo-crosslinking etc., were ambiguous or negative, and pointed only to a cryptic DNA binding [17]. Therefore, we have carried out a detailed quantitative analysis of DNA binding by DnaC protein using highly sensitive fluorescence anisotropy measurements and affinity-sensor analysis to conclusively resolve this issue.

First, we examined the interactions of DnaC protein with 5′-fluorescein-labelled 25 nt single stranded oligo(dT)$_{25}$ [Fl-oligo(dT)$_{25}$] at 23 °C and in buffer B containing 3.75 nM Fl-oligo(dT)$_{25}$, 25 mM KCl and 5 mM Mg^{2+}. The equilibrium DNA-binding by DnaC was measured by following increases in the anisotropy of the fluorescence of Fl-oligo(dT)$_{25}$ upon protein binding. Fluorescence anisotropy of Fl-oligo(dT)$_{25}$ was measured with titration of DnaC protein until a saturation in anisotropy was observed, the results are presented in Figure 2. The anisotropy values at various DnaC protein concentrations were used to create a binding isotherm as a semi-log plot (Figure 2). Analysis of the binding isotherm allowed determination of the thermodynamic parameters of DnaC–DNA binding [9,36,42,44]. The fluorescence anisotropy of Fl-oligo(dT)$_{25}$ alone was 50 ± 4 milli anisotropy

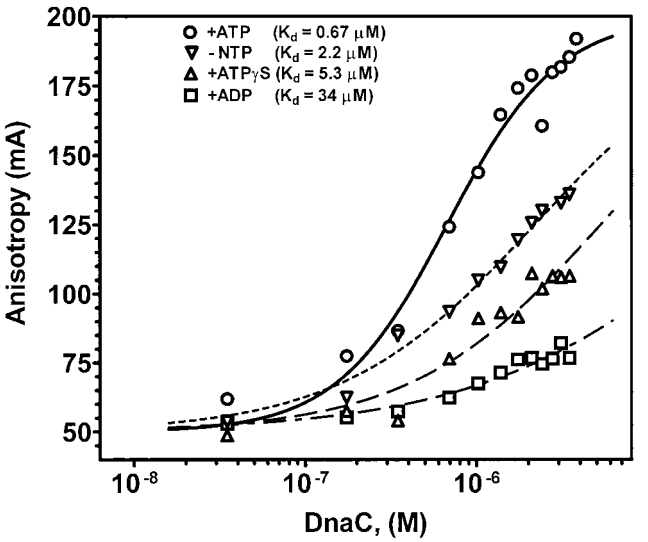

Figure 2 Effect of nucleotides on DnaC-ssDNA interaction

Titration of 3.75 nM Fl-oligo(dT)$_{25}$ oligonucleotide in the absence of nucleotides (▽) or the presence of 50 μM ATP (○), ATP[S] (ATPγS; △) or ADP (□). Buffer conditions were as described in the Materials and methods section. Temperature was held at 20 °C. Data for each titration were analysed by non-linear least-square-regression analysis using PRISM 3.0 from Graph pad Corporation, San Diego, CA, U.S.A.

Table 1 Equilibrium DNA binding parameters for DnaC protein

1 kcal ≡ 4.184 kJ; ATPγS, ATP[S].

Cofactors in DnaC • (dT)$_{25}$ complex formation	K_d (M)	$\Delta G°$ (kcal/mol)
DnaC + (dT)$_{25}$ ↔ [DnaC$_n$ • (dT)$_{25}$]	$2.2 \pm 0.04 \times 10^{-6}$	− 8.79
DnaC + (dT)$_{25}$ + ATP ↔ [ATP • DnaC$_n$ • (dT)$_{25}$]	$6.7 \pm 0.07 \times 10^{-7}$	− 9.60
DnaC + (dT)$_{25}$ + ATPγS ↔ [ATPγS • DnaC$_n$ • (dT)$_{25}$]	$5.3 \pm 0.06 \times 10^{-6}$	− 8.20
DnaC + (dT)$_{25}$ + ADP ↔ [ADP • DnaC$_n$ • (dT)$_{25}$]	$34 \pm 0.03 \times 10^{-6}$	− 6.90

(m*A*) units. At low DnaC concentrations ($< 1 \times 10^{-7}$ M), a small anisotropy change and a flat plateau (approx. 50 m*A*) was observed, which was attributed to the unbound or free Fl-oligo(dT)$_{25}$ [41]. Upon further titration of DnaC protein, the anisotropy value increased due to an increase in the DnaC • Fl-oligo(dT)$_{25}$ complex formation as shown in Figure 2. In the presence of 50 μM ATP and 5 mM Mg^{2+}, a sigmoidal binding isotherm with saturation binding at high DnaC protein concentration was observed. The maximum anisotropy of the complex was 185 m*A* units. Nonlinear regression analysis of the data computed the DnaC protein concentration at which 50 % of the ligand was in bound form (EC_{50}), which can be approximated to the apparent dissociation constant, K_d [36,41,44]. The fluorescence-emission intensity did not change significantly with increase in DnaC concentration (results not shown). Therefore, the anisotropy measurement during data collection was not affected by a change in fluorescence lifetime or scattered excitation light [44].

The binding of DnaC to DNA was relatively weak compared with other DNA-binding proteins such as DNA primase of *E. coli* [41]. However, these results clearly demonstrated the nucleotide dependence of DNA binding by DnaC protein. The K_d for DnaC • Fl-oligo(dT)$_{25}$ complex in the absence of nucleotide was 2.2×10^{-6} M (Figure 2, Table 1). The K_d of the complex in the

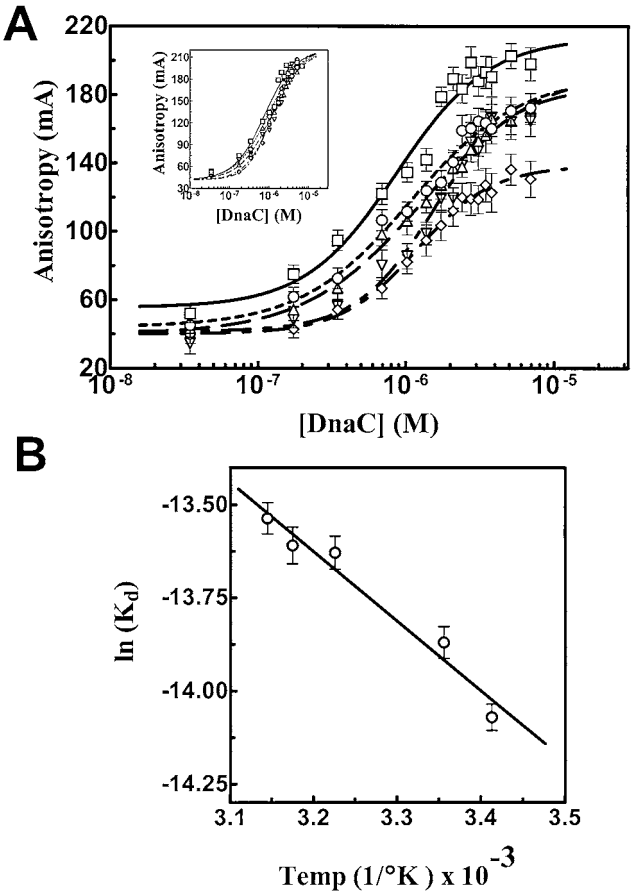

Figure 3 Thermodynamics of binding of DnaC protein to ssDNA

Titration of 3.75 nM Fl-oligo(dT)$_{25}$ oligonucleotide and 50 μM ATP at different temperatures. (**A**) shows fluorescence anisotropy data for the titration at: 20 °C (□), 25 °C (○), 30 °C (△) and 37 °C (◇). (**B**) shows the van't Hoff plot of the apparent K_d against the temperature. Buffer conditions were as described in the Materials and methods section. Data for each titration were analysed by least-square-regression analysis using PRISM 3.03 from Graphpad Corporation.

presence of ATP was 6.7×10^{-7} M. In the presence of ATP[S], the K_d was 5.3×10^{-6} M, which was significantly higher than that observed with ATP. DNA-binding analysis in the presence of ADP demonstrated an equally important nucleotide modulation of the DNA binding by DnaC. The K_d for DNA binding in the presence of ADP increased to 3.4×10^{-5} M (Figure 2). Thus, the dissociation constant decreased approx. 3-fold with ATP and increased approx. 17-fold with ADP, when compared with the dissociation constant in the absence of nucleotides. Therefore, DNA binding by DnaC appeared to be modulated approx. 79-fold by ATP and ADP as cofactors.

The effect of salt (ionic strength) was measured between 0 mM and 150 mM (results not shown). We observed saturation binding isotherms between 0–100 mM NaCl, although, the dissociation constant appeared to be lowest at 50 mM NaCl (results not shown). The dissociation constant increased with increase in ionic strength above 100 mM NaCl.

Temperature dependence and the thermodynamics of DNA binding

In order to delineate the thermodynamics of DnaC binding to DNA, we have analysed DNA binding as a function of temperature at 20 °C, 25 °C, 30 °C, and 37 °C. The binding isotherms for DnaC binding to Fl-oligo(dT)$_{25}$ are presented in Figure 3(A). Saturation of anisotropy plots for DNA binding was observed in this temperature range.

The binding isotherms were similar in nature at these temperatures; however, we observed an overall decrease in the anisotropy values of the free and bound oligonucleotides with increase in temperature. A similar decrease with temperature has been observed with oestrogen-receptor binding to oestrogen-responsive element and *E. coli* DNA primase binding to Fl-oligo(dT)$_{25}$ [36,41]. In both cases, the observed changes were attributed to a decrease in the viscosity with an increase in temperature. Therefore, the data were normalized for viscosity correction using the anisotropy values at 20 °C as standards in the case of Fl-oligo(dT)$_{25}$ (inset of Figure 3A). The dissociation constants of the DnaC • Fl-oligo(dT)$_{25}$ complex decreased steadily with temperature between 20 °C and 37 °C (Figure 3A).

The enthalpy change, derived from the van't Hoff plot (Figure 3B), was 2.6 ± 0.7 kcal/mol (where 1 cal $\equiv$ 4.184 J). The change in the entropy was found to be -19 ± 2.3 cal/°K per mol. Therefore, the association of DnaC with ssDNA appeared to be, in part, entropy driven.

Biosensor analysis of equilibrium DNA binding by DnaC protein

Equilibrium DNA binding was further analysed using an IAsys biosensor (Affinity Sensors Inc.). IAsys biosensor analysis has been used to study equilibrium protein–DNA and protein–protein interactions by several laboratories [39,40]. Synthetic 5′-biotinylated (dT)$_{30}$ oligonucleotides [biotin–oligo(dT)$_{30}$] were immobilized on the surface of a biotinylated biosensor chip using neutravidin (Pierce Biochemical Inc. Rockford, IL, U.S.A.). The biotin-coated biosensor surface was first saturated with a solution of neutravidin and the excess neutravidin was removed by repeated washing with buffer A. Biotin–oligo(dT)$_{30}$ was then added, incubated for 5 min and excess ligand was removed by several washings with buffer A. In order to measure DNA-binding kinetics, DnaC protein was added to the chip at various concentrations (3.4 nM to 5.2 μM in buffer B). The results of measurements at a number of different DnaC concentrations in the presence of 50 μM ATP are shown in Figure 4(A). Because of the low-affinity nature of the DNA binding, we did not observe any measurable DNA binding below 34 nM DnaC protein. Strong and measurable DnaC binding to the immobilized DNA was observed at or above 172 nM DnaC (Figure 4A).

In order to determine whether the observed nucleotide regulation of DNA binding by DnaC protein, can also be demonstrated by biosensor analysis of DnaC binding to immobilized DNA (as well as by fluorescence-anisotropy measurements), parallel measurements were carried out. The results of biosensor responses in the presence and absence of various nucleotides are shown in Figure 4(B). DNA binding was observed in the complete absence of nucleotides (−NTP). The binding was stimulated in the presence of ATP (50 μM), whereas the nonhydrolyzable ATP analogue, ATP[S], did not appear to alter DNA binding. Most importantly, DNA binding was significantly reduced in the presence of ADP. Thus, a direct correlation was apparent between the results of biosensor measurements (Figure 4B) and those obtained by fluorescence anisotropy (Figure 2), and established the pattern of nucleotide modulation of DNA binding by DnaC protein.

The maximum extents of DNA binding at each DnaC concentration in the absence of nucleotides, and in the presence of 50 μm ATP or ADP, were calculated and the data were fitted to the Hill equation using FastFit software (Figure 5). The values for the association rate constant (k_{on}) were calculated for each data set. Linear regression analysis of the plots of k_{on} versus the

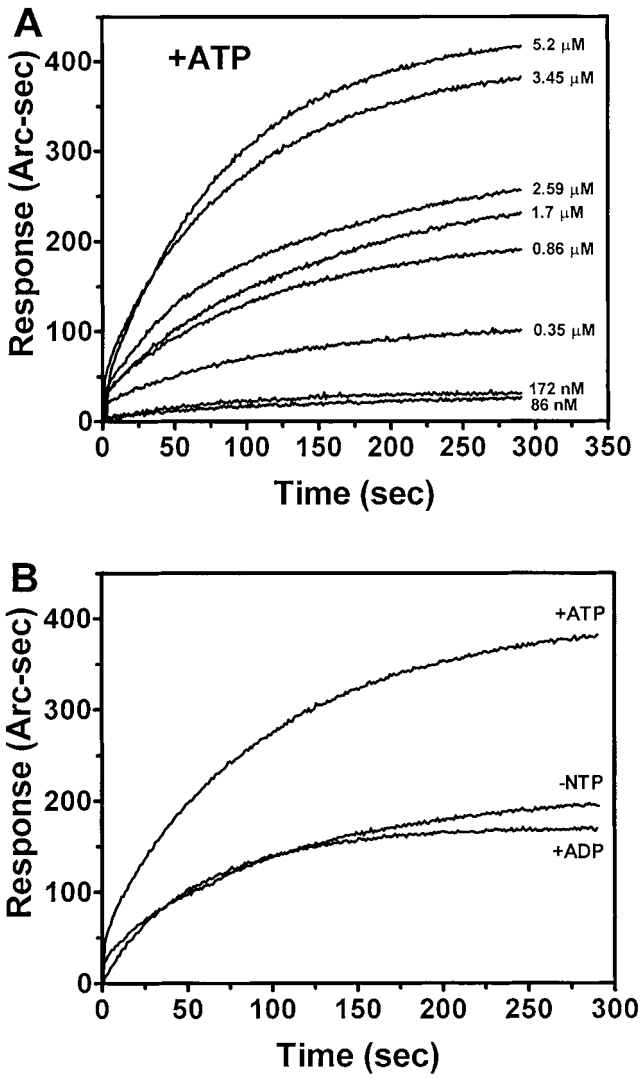

Figure 4 Affinity analysis of the kinetics of DnaC–ssDNA interaction

(**A**) Time-course analysis of oligo(dT)$_{30}$ binding in the presence of 50 μM ATP using various concentrations of DnaC. The extent of the binding was measured in arc s (arc-seconds). (**B**) Kinetics of ssDNA binding using 52 μM DnaC in the absence or presence of 50 μm ATP, ADP or no nucleotides (– NTP). Buffer conditions were as described in the Materials and methods section. Data for each titration were analysed using Fast plot and Fast fit software provided with the instrument.

concentration of DnaC resulted in straight lines. The apparent association rate constants (k_{ass}) were determined from the slopes, while the apparent dissociation rate constants (k_{diss}) were obtained from the intercepts (Table 2). K_d as calculated by: $K_d = k_{diss}/k_{ass}$ (Table 2).

Parameters of DNA binding by DnaC

The extent and rate of DNA binding was evaluated at each DnaC concentration using the plots in Figures 4 and 5. Binding parameters were calculated by using the FastFit program, and PRISM 3.03 program from GraphPad Software and the following equation (Table 2).

$$\text{(Extent bound) b} = (R_{max} \cdot S)/(K_d + S) \quad (2)$$

R_{max} is the maximum amount of response due to DnaC–DNA complex formation (the maximum extent of binding expressed

Table 2 Equilibrium DNA binding parameters for DnaC protein from biosensor analysis

The DnaC/(dT)$_{30}$ ratio was calculated on the basis of the calculated amount of 98.6 fmol of (dT)$_{30}$ bound to the total surface of the chip. NTP, nucleoside triphosphate.

Parameter	– NTP	ATP	ADP
B_{max} (Arc s)	512 ± 60	589 ± 74.5	450 ± 32
DnaC bound (fmol)	470	541	413
DnaC/(dT)$_{30}$ ratio	4.7 ± 0.5	5.5 ± 0.7	4.2 ± 0.3
K_{on} ($M^{-1} \cdot s^{-1}$)	1384 ± 347	3333 ± 572	646 ± 340
K_{off} (s^{-1})	.0084 ± 0.001	.0099 ± 0.001	.0086 ± 0.001
K_d (M)	6.1×10^{-6}	2.9×10^{-7}	1.3×10^{-5}

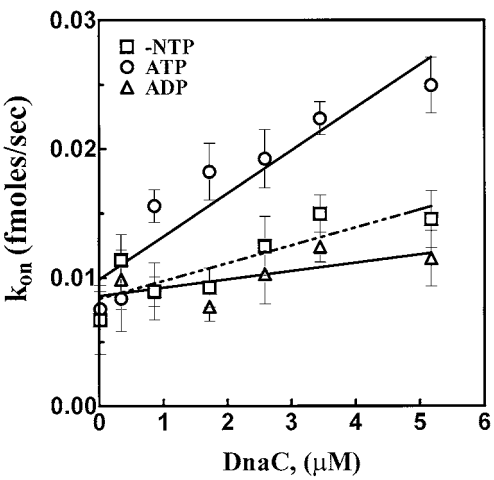

Figure 5 Multiple DnaC proteins bind to a single oligonucleotide

The maximum extents of ssDNA binding at each DnaC concentration in the absence of nucleotides (□), in the presence of 50 μm ATP (○), or ADP (△) were calculated and the data were fitted to the Hill equation using FastFit software, as described in the Materials and methods section. The values for k_{on} was calculated for each data set. A plot of k_{on} versus the concentration of DnaC results in straight lines that were derived by linear-regression analysis. The apparent association rate constant (k_{ass}) was obtained from the slope of the line, while the apparent dissociation rate constant (k_{diss}) was obtained from the intercept. K_d was calculated using the equation $K_d = k_{diss}/k_{ass}$.

in arc seconds), S is the free DnaC protein concentration and K_d represents an apparent dissociation constant. S was calculated by subtracting the amount of protein–DNA complex from total DnaC protein concentration. The amount of protein–DNA complex was determined using the information supplied by the manufacturer; i.e., that the biotinylated cuvettes used in this study have a useable surface area of 16 mm^2 and 600 arc seconds of response corresponds to 1 ng macromolecules bound/mm^2.

The total amount of biotinylated oligo(dT)$_{30}$ bound to the chip was 98.3 fmoles, as determined from the initial binding response (results not shown). Maximum DnaC binding, B_{max}, was determined by Fastfit analysis of the data. The B_{max} values in the presence and absence of nucleotides are shown in Table 2. The maximum binding of 541 fmoles of DnaC was observed in the presence of ATP. The association rate constant k_{on} increased in the presence of ATP and decreased significantly in the presence of ADP. The dissociation constants were 0.29 μM (+ATP), 13 μM (+ADP), and 6.1 μM in the absence of nucleotides (Table 2). In general, the results of the biosensor measurements appeared comparable with those from anisotropy analyses

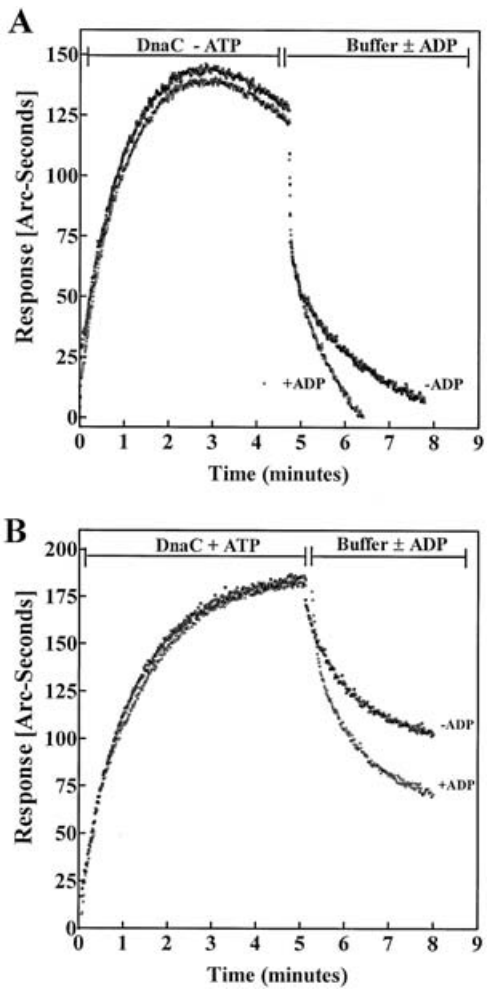

Figure 6 ADP-dependent dissociation of the DnaC-ssDNA complex

Biosensor analysis of DnaC binding to ssDNA, measured in either the presence (**A**) or absence (**B**) of ATP. Dissociation for both experiments were carried out with buffer alone or buffer containing ADP. In both cases, dissociation was significantly enhanced using buffer containing ADP.

(Table 1). The observed differences are relatively minor and could be due to the fact that the anisotropy measurements were direct equilibrium measurements, whereas biosensor measurements were strictly kinetic measurements. The dissociation constants in Table 2 were derived from the kinetic rates.

We have analysed the kinetic effects of ADP on the dissociation of DnaC • oligo(dT)$_{30}$ complex. The results are presented in Figure 6. In the absence of ATP, DnaC formed a complex with oligo(dT)$_{30}$. In the absence of ATP, the extent of binding of DnaC to oligo(dT)$_{30}$ was lower than that observed in the presence of ATP (Figures 6A and 6B). DnaC dissociates normally upon removal of excess DnaC using binding buffer. However, this complex appeared to dissociate more rapidly than that observed in the absence of ADP (Figure 6A). In the presence of ATP, a stable DnaC • oligo(dT)$_{30}$ complex was formed, which dissociated much slower upon removal of free DnaC than that observed in the absence of ATP (Figure 6B). However, in the presence of ADP, the dissociation rate of the DnaC • oligo(dT)$_{30}$ complex was enhanced. In both cases, these results indicated that ADP enhanced the rate of dissociation of DnaC • oligo(dT)$_{30}$ complex as well as the ATP • DnaC • oligo(dT)$_{30}$ ternary complex.

Stoichiometry of the DnaC • DNA complex

Fluorescence anisotropy studies (Figure 2) indicated that the anisotropy maximum, determined by nonlinear regression of the data, for the DnaC • DNA complex at saturating DnaC concentration and 50 μM ATP was approx. 200 m*A*. DnaC protein has a molecular mass of 29 kDa. The high anisotropy value of 200 m*A* with a small protein such as DnaC was unlikely due to a monomer or dimer binding to the Fl-oligo(dT)$_{25}$. For example, *E. coli* DnaG primase dimer (130 kDa) binding to Fl-oligo(dT)$_{25}$ leads to an anisotropy of approx. 125 m*A* [41] and that of *E. coli* DnaB hexamer (310 kDa) binding to Fl-oligo(dT)$_{25}$ leads to an anisotropy of approx. 230 m*A* (S. B. Biswas, unpublished work). Although, a quantitative correlation between size and anisotropy is difficult, it is apparent that a large number (approx. 5–10 protomers) of DnaC protein molecules can bind to a single Fl-oligo(dT)$_{25}$. Incidentally, multiple DnaC protein binding to a short ssDNA, parallels binding observed with other initiator proteins, for example, multiple protomers of DnaA protein, another *E. coli* replication initiator protein as well as an ATP/ADP switch, bind to the origin of DNA replication at *oriC* [3,6].

Quantification based on the B_{max} of 589 ± 75 arc seconds, derived from the affinity sensor analysis, indicated that the number of molecules of DnaC bound per molecule of oligo(dT)$_{30}$ was 5.5 ± 0.7 (Table 2). Assuming that DnaC probably bound DNA at a minimum as a dimer, it is possible that either three DnaC dimers or one quasi-hexamer of DnaC, bound a single DNA molecule. Thus, the results of biosensor measurements presented here correlated well with the results of anisotropy studies, as described above, and both point to the fact that multiple DnaC protomers bind a single DNA molecule, at least, in the presence of ATP.

Nucleotides and DNA modulate DnaB – DnaC protein interaction

The tryptophan residues are highly fluorescent internal probes in protein and these residues can function as unique internal reporters. We have examined the utilization of tryptophan fluorescence anisotropy to measure protein–protein interactions involving DnaB and DnaC proteins. We have studied the DnaB–DnaC interactions using a single-tryptophan mutant of DnaB (DnaBW48) where the other two native tryptophan residues (294 and 456) were mutated to Cys residues by *in vitro* mutagenesis, as described previously [45] and wild-type DnaC protein. We observed that total tryptophan anisotropy increases upon titration of DnaBW48 with DnaC protein. We have utilized this phenomenon to determine the apparent dissociation constant of $DnaB_6$ • $DnaC_6$ complex formation and to evaluate the probable roles of nucleotides and ssDNA.

The DnaB • DnaC complex formation was monitored by measuring anisotropy changes of the intrinsic tryptophan fluorescence of DnaB protein and titration with wild-type DnaC protein. The tryptophan fluorescence anisotropy of $DnaB_6$ was 130 m*A* and that of DnaC was 60 m*A* using 295 nm excitation wavelength (results not shown). First, anisotropy measurements clearly indicated that DnaB • DnaC complex could form in the complete absence of nucleotides (Figure 7). The binding isotherm was sigmoidal and saturable in the concentration range measured. The apparent dissociation constant was 3.5×10^{-7} M (Table 3). Next, we examined the effects of various adenine nucleotides to determine their modulatory effects on the complex formation. In the presence of ATP, ADP or ATP[S], the DnaB • DnaC complex formation was inhibited (Figure 7, Table 3). The extent of inhibition ranged from 3- to 10-fold. The modulation of the DnaB • DnaC complex formation by adenine nucleotides was

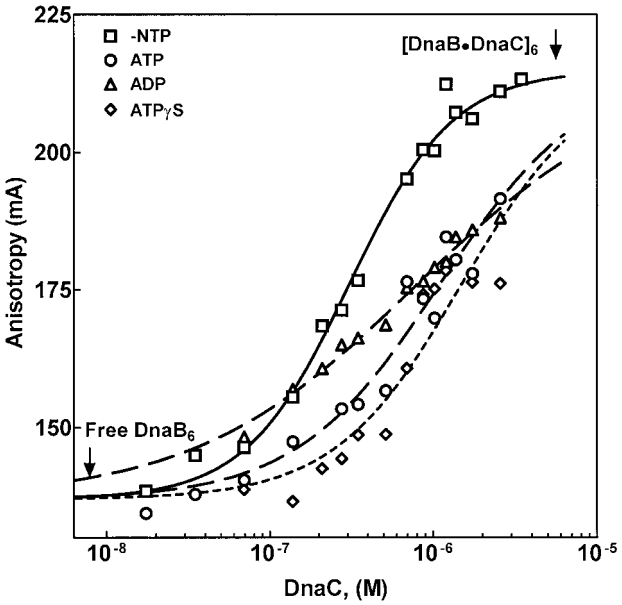

Figure 7 Nucleotides modulate interaction of DnaC protein with DnaB helicase

Changes in intrinsic tryptophan anisotropy of the single tryptophan mutant DnaBW48 (0.16 μM) was measured with an increasing concentration of DnaC in the absence of nucleotide substrate (□), in the presence of 50 μM each of ATP (○), ADP (△), or ATP[S] (◇). Titrations were carried out using standard fluorescence buffer at 20 °C, as described in the Materials and methods section. Data for each binding isotherm were analysed by non-linear least-square-regression analysis using PRISM 3.0 from Graph Pad Corporation, San Diego, CA, U.S.A.

Table 3 Binding constants for DnaC • DnaB complex with various cofactors

ATPγS, ATP[S].

Cofactors in $DnaB_6 \bullet DnaC_6$ complex formation	$K_{d,\,apparent}$ (M)
$DnaB_6 + 6DnaC \leftrightarrow [DnaB_6 \bullet DnaC_6]$	$(3.5 \pm 0.01) \times 10^{-7}$
$DnaB_6 + 6DnaC + ATP \leftrightarrow [DnaB_6 \bullet DnaC_6 \bullet ATP]$	$(17 \pm 0.05) \times 10^{-7}$
$DnaB_6 + (dT)_{25} + ATP\gamma S \leftrightarrow [DnaB_6 \bullet DnaC_6 \bullet ATP\gamma S]$	$(28 \pm 0.03) \times 10^{-7}$
$DnaB_6 + 6DnaC + ADP \leftrightarrow [DnaB_6 \bullet DnaC_6 \bullet ADP]$	$(10 \pm 0.07) \times 10^{-7}$
$DnaB_6 + 6DnaC + (dT)_{25} \leftrightarrow [DnaB_6 \bullet DnaC_6 \bullet (dT)_{25}]$	$(14 \pm 0.04) \times 10^{-7}$
$DnaB_6 + 6DnaC + (dT)_{25} + ATP \leftrightarrow [ATP \bullet DnaB_6 \bullet DnaC_6 \bullet (dT)_{25}]$	$(2.6 \pm 0.02) \times 10^{-7}$
$DnaB_6 + 6DnaC + (dT)_{25} + ADP \leftrightarrow [ADP \bullet DnaB_6 \bullet DnaC_6 \bullet (dT)_{25}]$	$(39 \pm 0.09) \times 10^{-7}$

remarkably different in the presence of oligo(dT)$_{25}$ (Figure 8). The DnaB • DnaC complex dissociation constant was 260 nM in the presence of ATP and oligo(dT)$_{25}$ whereas, the K_d increased 15-fold to 3.9 μM in the presence of ADP and oligo(dT)$_{25}$ (Figure 8, Table 3). Therefore, similar to DNA binding by DnaC, the $[DnaB \bullet DnaC]_6$ complex formation is also regulated by the nucleotides. Taken together, the conformations of DnaC protein associated with ATP and ADP forms are probably responsible for the 'on' (bound) or 'off' (dissociated) states of DnaC protein which affects similarly DNA and DnaB binding.

DISCUSSION

Intrinsic DNA-binding properties of DnaC protein

A cryptic ssDNA-binding activity of DnaC has been proposed previously, that may have considerable implication in the recruitment of DnaB helicase to the open complex at *oriC* [14,17].

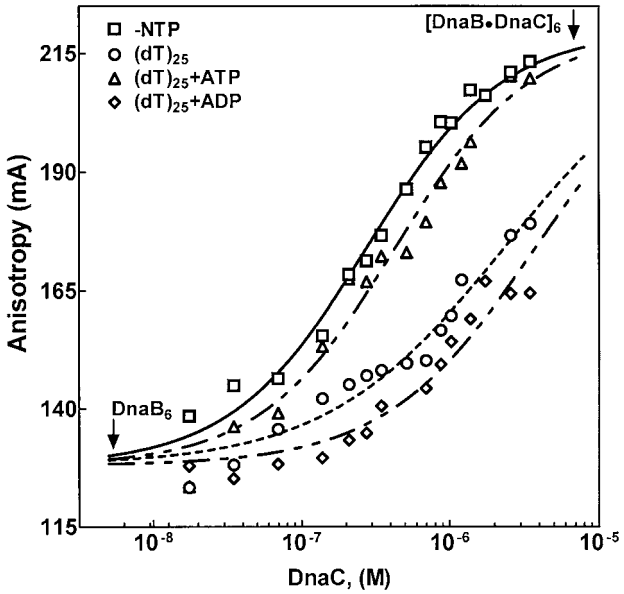

Figure 8 Modulation of interaction of DnaB and DnaC proteins by ssDNA

Changes in intrinsic tryptophan anisotropy of DnaB protein was measured with an increasing concentration of DnaC in the absence of substrates (□), in the presence of oligo(dT)$_{25}$ (○), oligo(dT)$_{25}$ + ADP (◇) or oligo(dT)$_{25}$ + ATP (△). Titrations were carried out using standard fluorescence buffer at 20 °C, as described in the Materials and methods section.

In order to establish ssDNA binding, as well as its mechanism and modulation by cofactors, we have employed two highly sensitive methods of analysing equilibrium DNA binding: fluorescence anisotropy and affinity sensor analysis.

DnaC protein, like many other members of the DNA-replication-initiator protein family, is an AAA+ ATPase [46]. Other members, such as DnaA protein of *E. coli*, origin recognition complex (ORC) protein subunits, and cdc6 of *Saccharomyces cerevisiae*, have varying degrees of ssDNA-binding abilities that are related to their highly specific roles in the initiation of DNA replication [24,47–51]. In many DNA-replication proteins that are involved in more extended roles in DNA replication, such as *E. coli* SSB (single-stranded DNA-binding protein), eukaryotic replication protein A etc., ssDNA binding is usually of high affinity [52]. The initiator proteins function in a transient manner in highly specific replicative roles; therefore, high affinity DNA binding is not a necessary prerequisite for replication initiator proteins. Fluorescence-anisotropy analysis of ssDNA binding by DnaC protein indicated that DnaC protein bound DNA with low to moderate affinities (Figure 2). Most importantly, the DNA-binding affinity was significantly modulated by the nucleotides. It bound DNA in the complete absence of any nucleotide. However, an optimal ssDNA binding was observed in the presence of ATP and not ATP[S] or ADP, as cofactors. The DNA-binding affinity decreased 50-fold when ATP was replaced with ADP. Differences in the conformations of DnaC • ATP and DnaC • ADP have recently been described, which would likely play a role in the observed differences in the binding affinities [53]. The affinity-sensor analysis of ssDNA binding produced results that mirrored the results of anisotropy analysis (Figures 5 and 6).

DNA binding is regulated by the ATP/ADP switch of DnaC protein

Like a classic ATP/ADP switch protein, DNA binding by DnaC protein is strictly modulated by the nucleotides, ATP and ADP. A moderate affinity and saturable equilibrium DNA binding was

observed only in the presence of ATP. Interestingly, the interaction of ATP and DnaC is highly specific and the nonhydrolyzable ATP analogue, ATP[S], did not appear to be able to replace ATP as a cofactor for DNA binding. In fact, both ATP[S] and ADP negatively modulated DNA binding compared with that observed in the absence of nucleotides, even though free DnaC does not appear to hydrolyze ATP in the complete absence of DnaB helicase [9,14]. The most important observation is that the DNA-binding affinity decreases 79-fold with change of cofactor from ATP to ADP. DnaC • ATP binds ssDNA and the concomitant formation of DnaC • ADP results in an immediate dissociation from DNA. The intracellular concentration of ATP is higher than ADP; therefore, DnaC protein should be in the predominantly ATP bound state. DnaC • ATP would bind ssDNA in the open complex of *oriC* with DnaA protein. However, the formation of ADP generated by ATPases such as DnaA, DnaB and other pre-primosomal proteins may increase the ADP concentration in the immediate vicinity of *oriC*, which may result in the displacement of ATP from the ATP • DnaC • ssDNA complex by ADP. Davey et al. [14] reported a very weak ATP hydrolysis by DnaC in the presence of DNA, which may also lead to the formation of ADP • DnaC • ssDNA complex. According to the results presented here, DnaC should dissociate rapidly from the resultant ADP • DnaC • ssDNA complex. In addition, a higher concentration of ADP, due to continuous ATP hydrolysis in the vicinity of the replication fork, would prevent reassociation of DnaC to the unwound ssDNA during the priming and elongation stages of *E. coli* DNA replication. Unlike DnaB helicase, DnaC is a very weak ATPase and not a mobile replication promoter, as a result, the ATP • DnaC • ssDNA complex would remain fixed for a prolonged time in the open complex until the pre-primosome is formed, due to the recruitment of DnaB and other proteins, and ADP is produced. We propose that ATP/ADP levels in the immediate vicinity of *oriC* and the replication fork modulate the functions of DnaC including DNA binding regardless of the cellular concentrations of ATP and ADP. The global cellular concentrations of ATP and ADP play a rather minor role.

Mechanism of DnaB • DnaC complex formation

DnaB helicase appears to interact with a number of other initiator proteins including DnaC, DnaG, DnaA, λP proteins [9,16,24,31,41,54]. Each of these interactions has a very specific role in the DNA replication. The DnaB • DnaC complex formation is pivotal to understanding the function of DnaC protein in *E. coli* chromosomal DNA replication. Kobori and Kornberg [31] first demonstrated the formation of an isolatable complex of DnaC protein with DnaB helicase. The stoichiometry of the complex is six DnaC monomers to one DnaB hexamer leading to a $DnaB_6 \cdot DnaC_6$ complex. This report describes the complex dynamics of DnaB and DnaC interaction in the presence of a host of cofactors that are present during initiation of replication in *oriC*, such as various nucleotides and DNA. The mechanism of interaction of DnaB and DnaC is also fundamental in deciphering the DnaC-assisted recruitment of DnaB to the open complex at *oriC*. Affinity-sensor analysis of DNA binding to DnaC indicated that approximately six monomers of DnaC bound to a single $(dT)_{30}$ molecule. The open complex at *oriC*, therefore, could be bound by multiple monomers or dimers of DnaC proteins. Therefore, we sought to analyse various modes of $DnaB_6 \cdot DnaC_6$ complex formation in the presence of various complexes of DnaC with different combinations of ATP, ADP, and DNA.

This report demonstrates that in the complete absence of nucleotides and DNA, DnaC and DnaB form the $DnaB_6 \cdot DnaC_6$ complex with an apparent dissociation constant of 3.5×10^{-7} M. However, this situation is possible only in an *in vitro* system and it is not possible at or near an active replication fork *in vivo* due to the presence of both ATP and ADP. Therefore, the formation of the $DnaB_6 \cdot DnaC_6$ complex will be modulated by the cofactors such as nucleotides and DNA. The results presented here demonstrate that individually ATP, ADP, ATP[S], and $oligo(dT)_{25}$ inhibited the $[DnaB \cdot DnaC]_6$ complex formation to a varying degree (Table 3, Figures 7 and 8). It was inhibited approximately 3-fold with ADP and 5-fold with ATP. A 4-fold inhibition was observed with $oligo(dT)_{25}$ alone. However, during DnaC mediated recruitment of DnaB to the open complex at *oriC*, the $DnaB_6 \cdot DnaC_6$ complex formation would take place in the presence of ssDNA and nucleotides. Therefore, we examined the complex formation in the presence of $oligo(dT)_{25}$ + ATP and $oligo(dT)_{25}$ + ADP. Results of these studies demonstrate that the complex formation is significantly modulated by nucleotides (Table 3, Figure 8). In the presence of $oligo(dT)_{25}$ and ATP, the dissociation constant was 2.6×10^{-7} M and it increased to 39×10^{-7} M in the presence of $oligo(dT)_{25}$ and ADP. The change in the equilibrium constant was 15-fold. Therefore, there will be a rapid and facile dissociation of the complex. However, the DnaB helicase forms a hexameric ring around the DNA, which is stable and therefore, would remain bound to the DNA. Consequently, the net result of hydrolysis of ATP to ADP in the [ATP • $DnaB_6$ • $DnaC_6$ • DNA] in *oriC* open complex would likely be the formation of the $DnaB_6$ • DNA, and the DnaC • ADP complex.

DnaC-assisted DnaB transfer to the oriC open complex and activation of the DNA helicase

DnaC protein binds to $DnaB_6$ hexamer in the N-terminal α domain as a trimer of three dimers [30]. Recent conformational analysis of DnaB protein, in complex with various substrates, indicates that the α domain appear to undergo major conformational changes during its catalytic cycle [45]. Electron microscopic studies clearly demonstrated the organization of the $[DnaB \cdot DnaC]_6$ complex. The complex is a ring of three DnaC dimers attached to the N-terminal α-domain face of the DnaB hexamer ring [30]. Therefore, in addition to inhibition of the ATPase activity of DnaB, DnaC may also block any conformational changes during the catalytic cycle of DnaB and thereby preventing the helicase function of DnaB.

The results of these studies are summarized in Figure 9. We have proposed here two possible avenues for the formation of [ATP • $DnaB_6$ • $DnaC_6$ • DNA] complex. One is through the formation of $[DnaB \cdot DnaC]_6$ complex followed by DNA binding in the presence of ATP and the other is through the formation of [ATP • $DnaC_n$ • ssDNA] complex and then assembly of $DnaB_6$ hexamer to the complex. Based on the thermodynamic data provided in this study, we propose the following mechanism of DnaB loading on to ssDNA by DnaC protein: (i) DnaC forms an apparent hexamer around the ssDNA to form [ATP • $DnaC_6$ • ssDNA]. (ii) DnaB hexamer slowly associates with the hexameric DnaC already bound to the DNA driven by the affinity of the two proteins for each other in the presence of ATP. (iii) During the completion of the DnaC • DnaB binding, ssDNA in the [ATP • $DnaC_6$ • ssDNA] complex slides through the subunit interface of the DnaB protomers. (iv) The energy that is required to pry open the DnaB • DnaB protomers interface, and ssDNA sliding into the hexamer is actually provided by the free energy of the DnaB-DnaC association leading to the formation of [ATP • $DnaC_6$ • ssDNA • $DnaB_6$] complex.

Once the [ATP • $DnaC_6$ • ssDNA • $DnaB_6$] complex is formed and ATP is hydrolyzed to ADP, the complex dissociates leaving the DnaB hexamer as a hexameric ring around the ssDNA

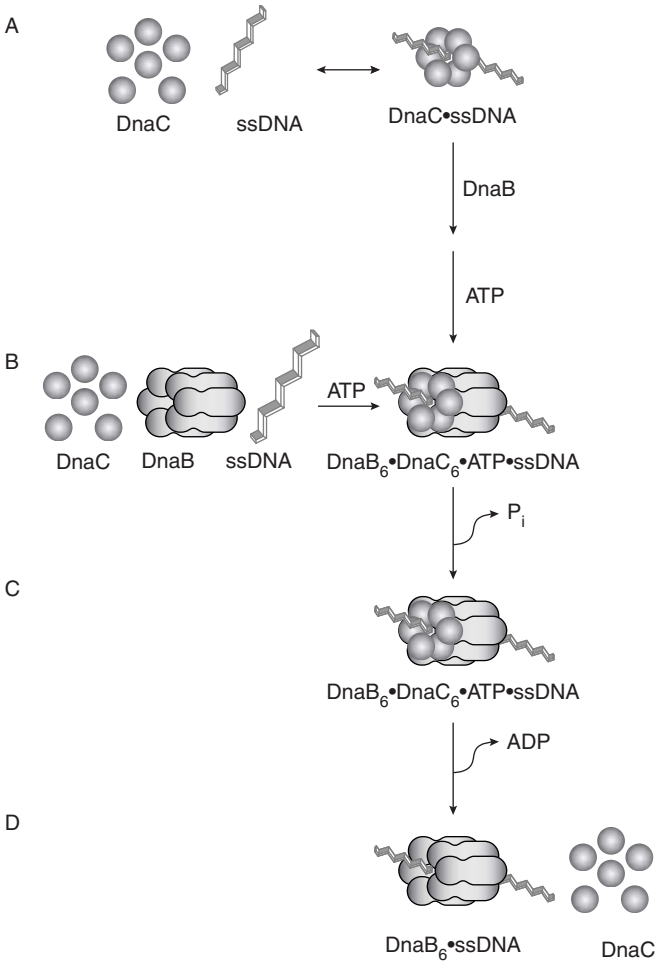

Figure 9 A proposed model depicting putative pathways of DnaC involvement in the DnaB helicase loading based on our finding of DnaC hexamer formation on ssDNA

(**A**) DnaC forms an apparent hexamer around the ssDNA to form [ATP • $DnaC_6$ • ssDNA]. (**B**) DnaB hexamer slowly associates with the hexameric DnaC already bound to the DNA driven by the affinity of the two proteins for each other in presence of ATP. During the completion of the DnaC • DnaB binding, ssDNA in the [ATP • $DnaC_6$ • ssDNA] complex slides through the subunit interface of the DnaB protomers. (**C**) The energy that is required to pry open the DnaB • DnaB protomers interface, and ssDNA sliding into the hexamer is actually provided by the free energy of the DnaB-DnaC association leading to the formation of [ATP • $DnaC_6$ • ssDNA • $DnaB_6$] complex. (**D**) Once the [ATP • $DnaC_6$ • ssDNA • $DnaB_6$] complex is formed and ATP is hydrolyzed to ADP, the complex dissociates leaving the DnaB hexamer as a hexameric ring around the ssDNA triggering the DNA-dependent ATPase of DnaB as well as the DNA helicase function. The complex, $DnaB_6$ • ssDNA is stable because of the lack of energy that is required to pry open DnaB • DnaB interface and sliding out the ssDNA.

triggering the DNA-dependent ATPase of DnaB as well as the DNA helicase function. The complex, $DnaB_6$ • ssDNA is stable because of the lack of energy that is required to pry open DnaB • DnaB interface and sliding out the ssDNA.

Velten et al. [33], demonstrated that in *B. subtilis* the corresponding DNA helicase is monomeric, forms a hexamer and is loaded on to the DNA by two helicase loaders, one monomeric like DnaC of *E. coli* and a second hexameric protein. In *E. coli*, the DnaB helicase is a stable hexamer and, therefore, may require a more rigorous loading mechanism involving transient ring opening. Consequently, the formation of a hexameric ring structure around the single-stranded DNA by DnaC monomers is required to facilitate transient ring opening, as well as loading, of the DnaB helicase according to the proposed mechanism. It is becoming apparent that hexameric helicases, as well as monomeric helicases that form hexamers, in different organisms have a number of different mechanisms for DNA helicase loading. The mechanism for DnaB helicase proposed here is one of them.

The authors wish to thank Dr Catherine A. Royer (Centre de Biochimie Structurale, INSERM, Montpellier, CEDEX 02, France) for the gift of BIOEQS software and training involving data analysis. We thank Dr Sujata Khopde of this laboratory for help with the data analysis, and Professor Robert Nagele of this department for critically reviewing this manuscript.

REFERENCES

1 Bramhill, D. and Kornberg, A. (1988) A model for initiation at origins of DNA replication. Cell (Cambridge, Mass.) **54**, 915–918
2 Kornberg, A. and Baker, T. A. (1992) DNA Replication. W. H. Freeman and Co., New York
3 Fuller, R. S., Funnell, B. E. and Kornberg, A. (1984) The DnaA protein complex with the *E. coli* chromosomal replication origin (oriC) and other DNA sites. Cell (Cambridge, Mass.) **38**, 889–900
4 Messer, W., Blaesing, F., Jakimowicz, D., Krause, M., Majka, J., Nardmann, J., Schaper, S., Seitz, H., Speck, C., Weigel, C. et al. (2001) Bacterial replication initiator DnaA. Rules for DnaA binding and roles of DnaA in origin unwinding and helicase loading. Biochimie **83**, 5–12
5 Konieczny, I. and Helinski, D. R. (1997) Helicase delivery and activation by DnaA and TrfA proteins during the initiation of replication of the broad host range plasmid RK2. J. Biol. Chem. **272**, 33312–33318
6 Bramhill, D. and Kornberg, A. (1988) Duplex opening by dnaA protein at novel sequences in initiation of replication at the origin of the E. coli chromosome. Cell (Cambridge, Mass.) **52**, 743–755
7 Allen, Jr, G. C. and Kornberg, A. (1991) Fine balance in the regulation of DnaB helicase by DnaC protein in replication in *Escherichia coli*. J. Biol. Chem. **266**, 22096–22101
8 Biswas, E. E., Biswas, S. B. and Bishop, J. E. (1986) The DnaB protein of *Escherichia coli*: mechanism of nucleotide binding, hydrolysis, and modulation by DnaC protein. Biochemistry **25**, 7368–7374
9 Biswas, S. B. and Biswas, E. E. (1987) Regulation of DnaB function in DNA replication in *Escherichia coli* by DnaC and λ P gene products. J. Biol. Chem. **262**, 7831–7838
10 Messer, W. and Weigel, C. (1996) in *Escherichia coli* and Salmonella: Cellular and Molecular Biology, 2nd ed. (Neidhart, F. C., ed.), pp. 1579–1601, ASM Press, Washington, D.C.
11 Wahle, E., Lasken, R. S. and Kornberg, A. (1989) The DnaB–DnaC replication protein complex of *Escherichia coli*. II. Role of the complex in mobilizing DnaB functions. J. Biol. Chem. **264**, 2469–2475
12 Wahle, E., Lasken, R. S. and Kornberg, A. (1989) The DnaB–DnaC replication protein complex of *Escherichia coli*. I. Formation and properties. J. Biol. Chem. **264**, 2463–2468
13 Doran, K. S., Helinski, D. R. and Konieczny, I. (1999) A critical DnaA box directs the cooperative binding of the *Escherichia coli* DnaA protein to the plasmid RK2 replication origin. J. Biol. Chem. **274**, 17918–17923
14 Davey, M. J., Fang, L., McInerney, P., Georgescu, R. E. and O'Donnell, M. (2002) The DnaC helicase loader is a dual ATP/ADP switch protein. EMBO J. **21**, 3148–3159
15 Marszalek, J. and Kaguni, J. M. (1994) DnaA protein directs the binding of DnaB protein in initiation of DNA replication in *Escherichia coli*. J. Biol. Chem. **269**, 4883–4890
16 Alfano, C. and McMacken, R. (1989) Ordered assembly of nucleoprotein structures. at the bacteriophage lambda replication origin during the initiation of DNA replication. J. Biol. Chem. **264**, 10699–10708
17 Learn, B. A., Um, S. J., Huang, L. and McMacken, R. (1997) Cryptic single-stranded-DNA binding activities of the phage λ P and *Escherichia coli* DnaC replication initiation proteins facilitate the transfer of *E. coli* DnaB helicase onto DNA. Proc. Natl. Acad. Sci. U.S.A. **94**, 1154–1159
18 LeBowitz, J. H. and McMacken, R. (1984) The bacteriophage λ O and P protein initiators promote the replication of single-stranded DNA. Nucleic Acids Res. **12**, 3069–3088
19 DePamphilis, M. L. (1998) Initiation of DNA replication in eukaryotic chromosomes. J. Cell. Biochem. Suppl. 30–31, 8–17
20 DePamphilis, M. L., Anderson, S., Bar-Shavit, R., Collins, E., Edenberg, H., Herman, T., Karas, B., Kaufmann, G., Krokan, H., Shelton, E. et al. (1979) Replication and structure of simian virus 40 chromosomes. Cold Spring Harb. Symp. Quant. Biol. **43**, 679–692
21 Stillman, B. (1994) Initiation of chromosomal DNA replication in eukaryotes. Lessons from λ. J. Biol. Chem. **269**, 7047–7050
22 Stillman, B. (1989) Initiation of eukaryotic DNA replication *in vitro*. **5**, 197–245
23 Stillman, B., Bell, S. P., Dutta, A. and Marahrens, Y. (1992) DNA replication and the cell cycle. Ciba Found Symp. **170**, 147–156; discussion 156–160

24 Liang, C., Weinreich, M. and Stillman, B. (1995) ORC and Cdc6p interact and determine the frequency of initiation of DNA replication in the genome. Cell (Cambridge, Mass,) **81**, 667–676
25 Bueno, A. and Russell, P. (1992) Dual functions of CDC6: a yeast protein required for DNA replication also inhibits nuclear division. EMBO J. **11**, 2167–2176
26 Yan, Z., DeGregori, J., Shohet, R., Leone, G., Stillman, B., Nevins, J. R. and Williams, R. S. (1998) Cdc6 is regulated by E2F and is essential for DNA replication in mammalian cells. Proc. Natl. Acad. Sci. U.S.A. **95**, 3603–3608
27 Mendez, J. and Stillman, B. (2000) Chromatin association of human origin recognition complex, cdc6, and minichromosome maintenance proteins during the cell cycle: assembly of prereplication complexes in late mitosis. Mol. Cell. Biol. **20**, 8602–8612
28 Kobori, J. A. and Kornberg, A. (1982) The *Escherichia coli* DnaC gene product. II. Purification, physical properties, and role in replication. J. Biol. Chem. **257**, 13763–13769
29 Kobori, J. A. and Kornberg, A. (1982) The *Escherichia coli* dnaC gene product. I. Overlapping of the DnaC proteins of *Escherichia coli* and *Salmonella typhimurium* by cloning into a high copy number plasmid. J. Biol. Chem. **257**, 13757–13762
30 Barcena, M., Ruiz, T., Donate, L. E., Brown, S. E., Dixon, N. E., Radermacher, M. and Carazo, J. M. (2001) The DnaB–DnaC complex: a structure based on dimers assembled around an occluded channel. EMBO J. **20**, 1462–1468
31 Kobori, J. A. and Kornberg, A. (1982) The *Escherichia coli* DnaC gene product. III. Properties of the DnaB–DnaC protein complex. J. Biol. Chem. **257**, 13770–13775
32 San Martin, M. C., Stamford, N. P., Dammerova, N., Dixon, N. E. and Carazo, J. M. (1995) A structural model for the *Escherichia coli* DnaB helicase based on electron microscopy data. J. Struct. Biol. **114**, 167–176
33 Velten, M., McGovern, S., MArsin, S., Ehrlich, S., Noirot, P. and Polard, P. (2003) A two-protein strategy for the functional loading of a cellular replicative DNA helicase. Mol. Cell **11**, 1009–1020
34 Mitkova, A., Khopde, S. and Biswas, S. (2003) Mechanism and stoichiometry of interaction of DnaG primase and DnaB helicase of *Escherichia coli* in RNA primer synthesis. J. Biol. Chem. **278**, 52253–52261
35 Margeat, E., Bourdoncle, A., Margueron, R., Poujol, N., Cavailles, V. and Royer, C. (2003) Ligands differentially modulate the protein interactions of the human oestrogen receptors α and β. J. Mol. Biol. **326**, 77–92
36 Boyer, M., Poujol, N., Margeat, E. and Royer, C. A. (2000) Quantitative characterization of the interaction between purified human oestrogen receptor α and DNA using fluorescence anisotropy. Nucleic Acids Res. **28**, 2494–2502
37 Royer, C. A. and Beechem, J. M. (1992) Numerical analysis of binding data: advantages, practical aspects, and implications. Methods Enzymol. **210**, 481–505
38 Gryczynski, I., Steiner, R. F. and Lakowicz, J. R. (1991) Intensity and anisotropy decays of the tyrosine calmodulin proteolytic fragments, as studied by GHz frequency-domain fluorescence. Biophys. Chem. **39**, 69–78
39 De Zutter, J. K. and Knight, K. L. (1999) The hRad51 and RecA proteins show significant differences in cooperative binding to single-stranded DNA. J. Mol. Biol. **293**, 769–780
40 Zylicz, M., King, F. W. and Wawrzynow, A. (2001) Hsp70 interactions with the p53 tumour suppressor protein. EMBO J. **20**, 4634–4638
41 Khopde, S., Biswas, E. E. and Biswas, S. B. (2002) Affinity and sequence specificity of DNA binding and site selection for primer synthesis by *Escherichia coli* primase. Biochemistry **41**, 14820–14830
42 LeTilly, V. and Royer, C. A. (1993) Fluorescence anisotropy assays implicate protein–protein interactions in regulating trp repressor DNA binding. Biochemistry **32**, 7753–7758
43 Royer, C. A., Smith, W. R. and Beechem, J. M. (1990) Analysis of binding in macromolecular complexes: a generalized numerical approach. Anal. Biochem. **191**, 287–294
44 Lakowicz, J. R. (1999) Principles of fluorescence spectroscopy, 2nd ed., Plenum Publishers, New York, NY 10013
45 Flowers, S., Biswas, E. E. and Biswas, S. (2003) Conformational dynamics of DnaB helicase upon DNA and nucleotide binding: analysis by intrinsic tryptophan fluorescence quenching. Biochemistry **42**, 1910–1921
46 Koonin, E. V. (1992) DnaC protein contains a modified ATP-binding motif and belongs to a novel family of ATPases including also DnaA. Nucleic Acids Res. **20**, 1997
47 Perkins, G. and Diffley, J. F. (1998) Nucleotide-dependent prereplicative complex assembly by Cdc6p, a homolog of eukaryotic and prokaryotic clamp-loaders. Mol. Cell **2**, 23–32
48 Bell, S. P., Mitchell, J., Leber, J., Kobayashi, R. and Stillman, B. (1995) The multidomain structure of Orc1p reveals similarity to regulators of DNA replication and transcriptional silencing. Cell (Cambridge, Mass.) **83**, 563–568
49 Bell, S. P. and Stillman, B. (1992) ATP-dependent recognition of eukaryotic origins of DNA replication by a multiprotein complex. Nature (London) **357**, 128–134
50 Dhar, S. K., Delmolino, L. and Dutta, A. (2001) Architecture of the human origin recognition complex. J. Biol. Chem. **276**, 29067–29071
51 Li, Y. F., Kim, S. T. and Sancar, A. (1993) Evidence for lack of DNA photoreactivating enzyme in humans. Proc. Natl. Acad. Sci. U.S.A. **90**, 4389–4393
52 Hey, T., Lipps, G. and Krauss, G. (2001) Binding of XPA and RPA to damaged DNA investigated by fluorescence anisotropy. Biochemistry **40**, 2901–2910
53 Galletto, R. and Bujalowski, W. (2002) The E. coli replication factor DnaC protein exists in two conformations with different nucleotide binding capabilities. I. Determination of the binding mechanism using ATP and ADP fluorescent analogues. Biochemistry **41**, 8907–8920
54 Marszalek, J., Zhang, W., Hupp, T. R., Margulies, C., Carr, K. M., Cherry, S. and Kaguni, J. M. (1996) Domains of DnaA protein involved in interaction with DnaB protein, and in unwinding the *Escherichia coli* chromosomal origin. J. Biol. Chem. **271**, 18535–18542

Received 15 August 2003/20 December 2003; accepted 9 January 2004
Published as BJ Immediate Publication 9 January 2004, DOI 10.1042/BJ20031255